NOAA Technical Report ERL 389-SEL 38

A Division of the *aa* Indices Into Six Classes Based on the *Ap* Index, 1868–1976

Joseph A. Sutorik
Cheryl M. Cruickshank

July 1977

U.S. DEPARTMENT OF COMMERCE
National Oceanic and Atmospheric Administration
Environmental Research Laboratories

NOAA Technical Report ERL 389–SEL 38

A Division of the *aa* Indices Into Six Classes Based on the *Ap* Index, 1868–1976

Joseph A. Sutorik
Cheryl M. Cruickshank

Space Environment Laboratory
Boulder, Colorado

July 1977

U.S. DEPARTMENT OF COMMERCE
Juanita Kreps, Secretary

National Oceanic and Atmospheric Administration
Richard A. Frank, Administrator

Environmental Research Laboratories
Wilmot Hess, Director

Contents

A Division of the *aa* Indices Into Six Classes Based on the *Ap* Index, 1868–1976

Joseph A. Sutorik
Cheryl M. Cruickshank

Abstract. By using contingency table evaluation, Mayaud's *aa* indices of 1868–1967 are converted into six classes based on the *Ap* index. Five of the divisions are for days when the geomagnetic *Ap* intensity was ≥ 15. The published *Ap* values of 1968–1976 are also converted into these same class divisions. These data provide a 109-year history of the geomagnetic field for active- or storm-day conditions. An analysis of the 109-year record suggests that coronal holes have occurred in each of the last 10 solar cycles. Though coronal holes predominantly appear in the declining years of a solar cycle, they may appear throughout a cycle. In addition the study analyzes monthly, annual, and solar cycle distributions and predicts a course for solar cycle 21.

1. Introduction

Numerous magnetic indices (Bartels, 1957; Lincoln, 1967; Rostoker, 1972) have been developed through the years. However, the spatial and temporal response of the geomagnetic field (Russell, 1975; Svalgaard, 1975), as measured by a specific geomagnetic index, presents difficulties in defining an accurate and continuous history of solar and geomagnetic relationships. A linear function, such as the *Ap* index, provides a description of the daily state of geomagnetic activity. The *aa* indices (Mayaud, 1973) provide a scaled measurement of geomagnetic activity since 1868. By their singular (antipodal) nature, these indices are appropriate for statistical conversion based on the *Ap* index.

Values for *Ap*, the index of daily equivalent planetary amplitude (Bartels, 1957), are available back to 1932 in the International Association for Geomagnetism and Aeronomy (IAGA) bulletin series. The quasi-logarithmic 3-hour range *K* index (Bartels et al., 1939) and the equivalent range *ak* index (Table 1) are used to obtain the daily index *Ak* for portions of the data base. Both *ak* and *Ak* are linear measures; *Ak*, the index of equivalent daily amplitude for a single geomagnetic station, is the average of the sum of the eight daily *ak* values.

Table 1. Equivalent Range *ak* for Given *K*

K	0	1	2	3	4	5	6	7	8	9
ak	0	3	7	15	27	48	80	140	240	400

The purpose of this study is to provide a simple numerical value to describe the average daily state of the geomagnetic field. A regression line obtained from a correlation of the *aa* and *Ap* indices will provide a daily value; however, it would be difficult to evaluate, since these values for *Ap* may range between 0 and nearly 300. For this reason, contingency table methodology is used to provide discrete levels or class divisions (see section 2.1). These divisions of the *aa* indices extend the concept of the more familiar *Ap* index from 1932 back to 1868. A value defining the average daily state of the geomagnetic field is made available, thus allowing analysis of monthly, annual, or solar cycle distribution and recurrent patterns (M-regions) for the past 10 solar cycles. The recurrent patterns are used to infer the time periods for the existence of coronal holes.

2. Data Base

To provide a suitable data base to be used as a criterion for correlation, 293 geomagnetic days were selected between 1937 and 1967. Selection was made within the following ordered guidelines:

(1) Selection of data over several solar cycles to reduce chance bias due to any magnetic response that is characteristically inherent within a solar cycle (Abdel-Wahab and Goned, 1974).

(2) Selection of a sufficient number of data points to provide a suitable distribution for the entire spectrum of geomagnetic response.

(3) Selection within each solar cycle of a series of sequential days with varying degrees of geomagnetic disturbance. This selection was made to reduce bias due to diurnal response characteristics (Cage and Zawalik, 1972).

(4) Selection of values throughout the year to reduce bias due to the "semiannual wave" (Chapman and Bartels, 1940; McIntosh, 1959; Bartels, 1963; Russell and McPherron, 1973, 1974).

Three daily magnetic indices are included for correlative evaluation. The first is the average value of the *aa* indices for the northern (N) and southern (S) antipodal stations. In the averaging process, all half values are rounded to the next higher integer; this index will be referred to as $\overline{aa}$. The second index is the *Ap* value. The third index is the *Ak* value obtained from Cheltenham, Maryland, through May 1956 and from Fredericksburg, Virginia, after November 1956. For the period 1937–1946, the *Ak* values for Cheltenham were obtained by averaging the eight *ak* values corresponding to the published *K*-index. Because of the proximity of Cheltenham and Fredericksburg, their values are used in the data base as one station and referred to as *Afr*. A list of the indices used for the data base and their sources constitute the Appendix.

2.1 Derivation of Class Divisions

By following the above guidelines for data base selection, a distribution is provided for correlative evaluation of the three selected magnetic indices. Computer-generated video displays showing the distribution for the intercomparison of these three indices are shown in

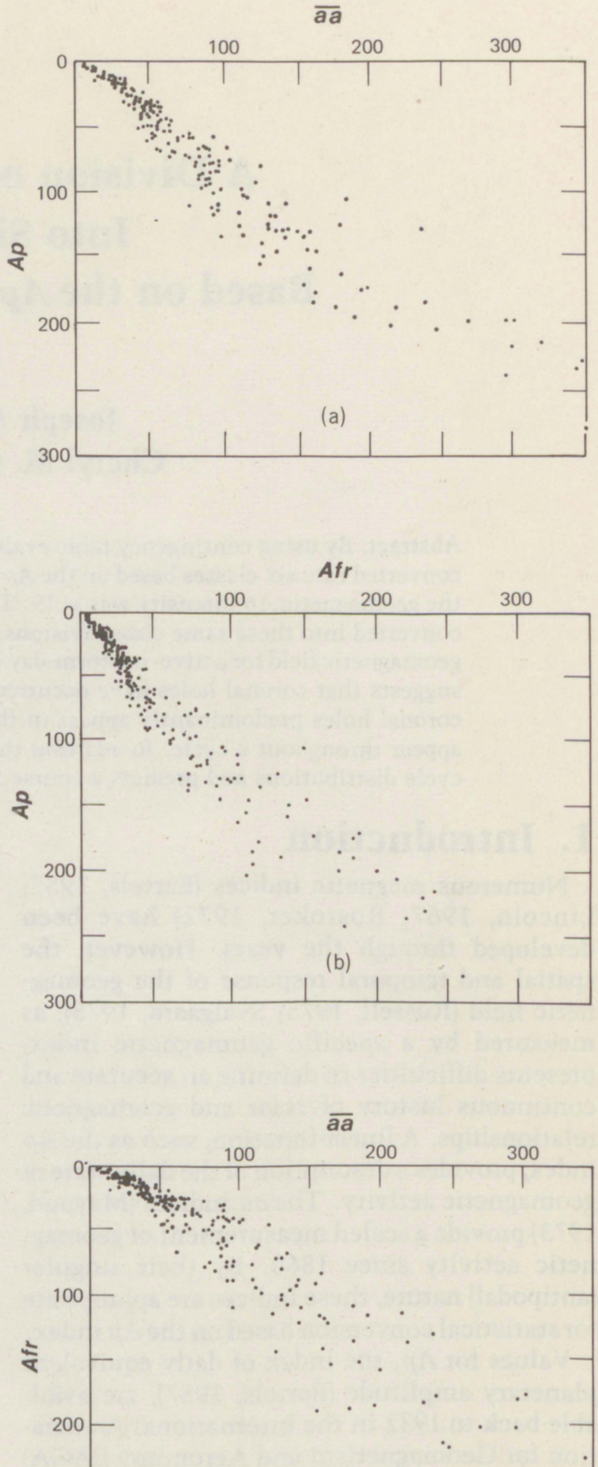

Figure 1. Computer-generated video display of the data base showing distribution for comparison of the three indices: (a) Ap–$\overline{aa}$; (b) Ap–Afr; and (c) Afr–$\overline{aa}$.

Figure 1. A "shotgun" pattern (distribution diverging from the source) is evident for all three comparisons. Least-squares curve fitting was accomplished by computer. The regression line equation derived for the Ap–$\overline{aa}$ indices was found to be

$$Ap = 1.8 + 0.8\overline{aa}$$

with the index of determination = 0.917.

Because the regression line provides finite daily values difficult to analyze, its use was abandoned in favor of a contingency table evaluation. In a contingency table, the data are gridded into appropriate sets of boxes. The boundary values for one parameter are fixed, whereas the boundary values of the second parameter are derived to obtain the best-fit distribution for the two parameters. For example, in Figure 2 the first limiting value of 29 for $\overline{aa}$ is derived to produce zero occurrences in boxes B, C, . . ., when $0 \le Ap < 15$. Similarly, the second limiting value of 50 for $\overline{aa}$ is derived to produce zero occurrences in boxes C, D, . . ., when $15 \le Ap < 30$. This method is used to derive the limiting values for the entire contingency table. Ideally, the number of occurrences should be in the set of boxes running diagonally across the contingency table. This is not possible for all divisions; therefore, some degree of compromise is necessary. In this paper, emphasis was placed on minimizing the number of occurrences below the set of diagonal boxes.

Figure 2 shows the distribution of the data base and the boundary values obtained when the Ap and $\overline{aa}$ indices are compared. These boundary values will later be used to assign a class division for each geomagnetic day beginning in 1868 (see Table 2). Figures 3 and 4 show the distribution comparing Ap–Afr and Afr–$\overline{aa}$, respectively. The limiting values for the distribution between Afr and $\overline{aa}$ were determined by the values obtained for the Ap–$\overline{aa}$ and the Ap–Afr contingency tables. Adams (1975) provides a detailed evaluation of the comparison of Ap and Afr. No further evaluation for a midlatitude station will be made in this paper.

In Figures 2, 3, and 4, the upper value in each box shows the number of occurrences within the designated limits of the two indices; the lower value is the ratio of the upper value to total occurrences for that column, expressed as a percentage.

Ap \ $\overline{aa}$	A	B	C	D	E	F
a	36 69%	0	0	0	0	0
b	16 31%	43 57%	0	0	0	0
c	0	31 41%	35 58%	0	0	0
d	0	2 3%	25 42%	34 74%	2 5%	0
e	0	0	0	12 26%	36 92%	1 10%
f	0	0	0	0	1 3%	9 90%

where

A: $0 \le \overline{aa} < 29$
B: $29 \le \overline{aa} < 50$
C: $50 \le \overline{aa} < 74$
D: $74 \le \overline{aa} < 118$
E: $118 \le \overline{aa} < 245$
F: $245 \le \overline{aa} < 400$

a: $0 \le Ap < 15$ = class 0
b: $15 \le Ap < 30$ = class 1
c: $30 \le Ap < 50$ = class 2
d: $50 \le Ap < 100$ = class 3
e: $100 \le Ap < 200$ = class 4
f: $200 \le Ap < 400$ = class 5

Figure 2. Contingency table for Ap and $\overline{aa}$ indices.

2.2 Test of the Limiting Values

An independent sample was selected to determine the degree of confidence that could be obtained when the limiting values of the contingency table are applied to this sample for the different levels of activity. This sample is composed of the daily values of $\overline{aa}$ and Ap for the period 1960 through 1967. Excluded from the sample are the days that were included in

Table 2. Geomagnetic Field Classification

Class	Ap Index	Definition
0	$0 \le Ap < 7$	Quiet, usually no K-indices > 2
0	$7 \le Ap < 15$	Unsettled, usually no K-indices > 3
1	$15 \le Ap < 30$	Active, a few K-indices of 4
2	$30 \le Ap < 50$	Minor Storm, K-indices mostly 4 & 5
	$Ap \ge 50$	Major Storm, some K-indices 6 or greater
	Added by this study:	
3	$50 \le Ap < 100$	
4	$100 \le Ap < 200$	
5	$Ap \ge 200$	

Ap \ Afr	A	B	C	D	E	F
a	31 78%	5 7%	0	0	0	0
b	9 22%	47 70%	3 5%	0	0	0
c	0	14 21%	49 69%	3 5%	0	0
d	0	1 2%	19 27%	41 73%	2 5%	0
e	0	0	0	12 22%	36 88%	1 12%
f	0	0	0	0	3 7%	7 88%

where

A: $0 \le Afr < 13$ a: $0 \le Ap < 15$
B: $13 \le Afr < 26$ b: $15 \le Ap < 30$
C: $26 \le Afr < 39$ c: $30 \le Ap < 50$
D: $39 \le Afr < 82$ d: $50 \le Ap < 100$
E: $82 \le Afr < 200$ e: $100 \le Ap < 200$
F: $200 \le Afr < 400$ f: $200 \le Ap < 400$

Figure 3. Contingency table for *Ap* and *Afr* indices.

Afr \ $\overline{aa}$	A	B	C	D	E	F
a	35 67%	5 7%	0	0	0	0
b	17 33%	45 59%	5 8%	0	0	0
c	0	25 33%	42 70%	4 9%	0	0
d	0	1 1%	13 22%	36 78%	6 15%	0
e	0	0	0	6 13%	33 85%	2 20%
f	0	0	0	0	0	8 80%

where

A: $0 \le \overline{aa} < 29$ a: $0 \le Afr < 13$
B: $29 \le \overline{aa} < 50$ b: $13 \le Afr < 26$
C: $50 \le \overline{aa} < 74$ c: $26 \le Afr < 39$
D: $74 \le \overline{aa} < 118$ d: $39 \le Afr < 82$
E: $118 \le \overline{aa} < 245$ e: $82 \le Afr < 200$
F: $245 \le \overline{aa} < 400$ f: $200 \le Afr < 400$

Figure 4. Contingency table for *Afr* and $\overline{aa}$ indices.

the data base. This test sample of 2,869 geomagnetic days includes the last 5 years of cycle 19 and the first 3 years of cycle 20.

Figure 5 shows the distribution of the test sample when the limiting values from the contingency table for Ap–$\overline{aa}$ are applied to the sample. The largest variation in the level of Ap activity for a given interval of $\overline{aa}$ values was in the intermediate range where $50 \le \overline{aa} < 74$. In this range, 10% of the values fell below the level desired for comparison with the Ap index ($Ap \ge 30$). The original concept was to maintain a minimum number of occurrences below a specified class level in the transfer of the $\overline{aa}$ indices into class divisions. As a result of this "worst case" obtained from the large test sample we estimate that at least a 90% confidence level has been established for the conversion of the $\overline{aa}$ indices into a class division equal to or greater than the desired value. This numerical definition of the average daily state of the geomagnetic field provides a simple, homogeneous set of values for studying the occurrence and distribution of active- or storm-days for 109 years spanning 10 solar cycles.

3. Background Review of Recurrent Geomagnetic Activity and Coronal Holes

The cyclic nature of the Sun and of geophysical parameters has long been identified. Bartels (1932, 1934) identified the periodic recurrent patterns of the geomagnetic field (M-regions). Allen (1944) quite accurately defined the concepts currently believed to be the cause of recurrent geomagnetic activity:

> Some properties of M-regions can be gathered by a study of the 27-day charts. Referring to the chart for 1923–1933 (*Terr. Mag.*, **37**, 1, 1932; **39**, 201, 1934), we see that the M-regions sometimes persist for a year or more, and that they frequently continue through periods of complete sunspot inactivity. It is evident that spots are not necessary to their existence. Another feature of some significance is that there are nearly always two or three M-regions on the Sun at a time, and the disappearance of an M-region often synchronizes with the appearance of another. This feature makes it probable that the M-region is not a small area coming into activity by some fortuitous

Ap \ $\overline{aa}$	A	B	C	D	E	F
a	2115 93%	21 5%	0	0	0	0
b	155 7%	378 82%	11 10%	0	0	0
c	0	63 14%	70 65%	1 4%	0	0
d	0	0	27 25%	23 85%	0	0
e	0	0	0	3 11%	2 100%	0
f	0	0	0	0	0	0

where

A: $0 \leq \overline{aa} < 29$	a: $0 \leq Ap < 15$ = class 0
B: $29 \leq \overline{aa} < 50$	b: $15 \leq Ap < 30$ = class 1
C: $50 \leq \overline{aa} < 74$	c: $30 \leq Ap < 50$ = class 2
D: $74 \leq \overline{aa} < 118$	d: $50 \leq Ap < 100$ = class 3
E: $118 \leq \overline{aa} < 245$	e: $100 \leq Ap < 200$ = class 4
F: $245 \leq \overline{aa} < 400$	f: $200 \leq Ap < 400$ = class 5

Figure 5. Distribution in the test sample of the *Ap*–$\overline{aa}$ indices based on the contingency table limiting values.

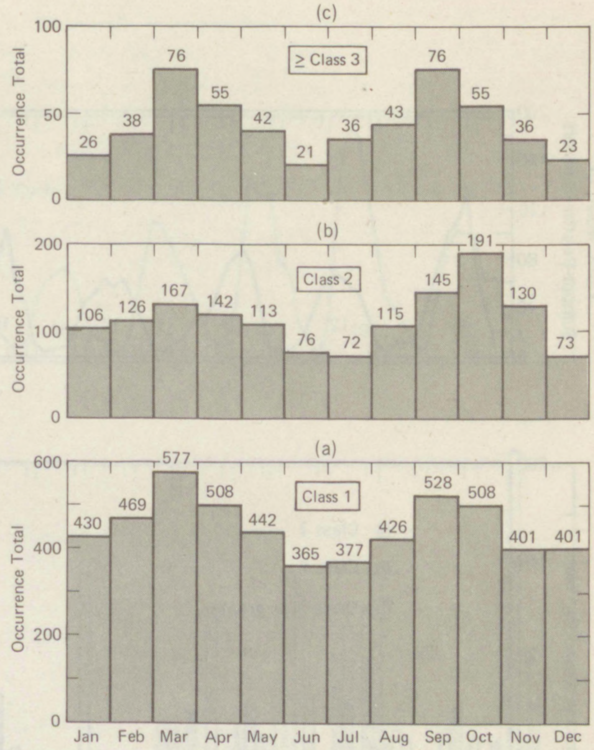

Figure 6. Monthly distribution for (a) active conditions (class 1); (b) minor-storm conditions (class 2); and (c) major-storm conditions (≥ class 3) for the period 1868–1976.

chance like a sunspot. It is more likely to be an emission coming continuously from practically the whole of the Sun's surface and constrained to move in streams by forces in the Sun's atmosphere. It would then be the continuity of these streams that cause the persistence and changes of the recurrent magnetic storms.

With the advent of the space age, the solar-interplanetary sector structure was defined (Wilcox, 1968). Continued scientific advances provided the magnificent photographs of solar coronal holes. The relationship between coronal holes and attendant high-speed solar wind streams was discussed by Kreiger et al. (1973). Sheeley et al. (1976) provided a review of the interaction of coronal holes, high-speed wind streams, and the geomagnetic field for the 1973–1976 period.

In a 1971 study, 01′ discusses the relationship he discovered between the recurrent geomagnetic activity during the declining branch of a solar cycle and the maximum relative sunspot number for the next solar cycle. This relationship shows that the maximum relative sunspot number of a solar cycle is directly related to the intensity of the recurrent geomagnetic activity in the declining branch of the preceding cycle.

4. The 109-Year Record: Analysis and Evaluation

On the basis of the conversion values established by the contingency distribution table (Figure 2), Mayaud's (1973) measured antipodal values are divided into six classes, of which five define active- or storm-day conditions (Table 2). (The definition for the state of the geomagnetic field as related to the *Ap* value is stated in the International Ursigram and World Days Service [IUWDS] Circular Letter RWC–123, dated June 1, 1971.) Class divisions 3, 4, and 5 have been added to provide more information when $Ap \geq 50$ (major storms). To make the study current, *Ap* values for 1968–1976 were taken from the NOAA/EDS Solar-Geophysical Data report series and converted into the class division format. Daily class values for the period 1868–1976 are available in catalog format (Sutorik and Cruickshank, 1977).

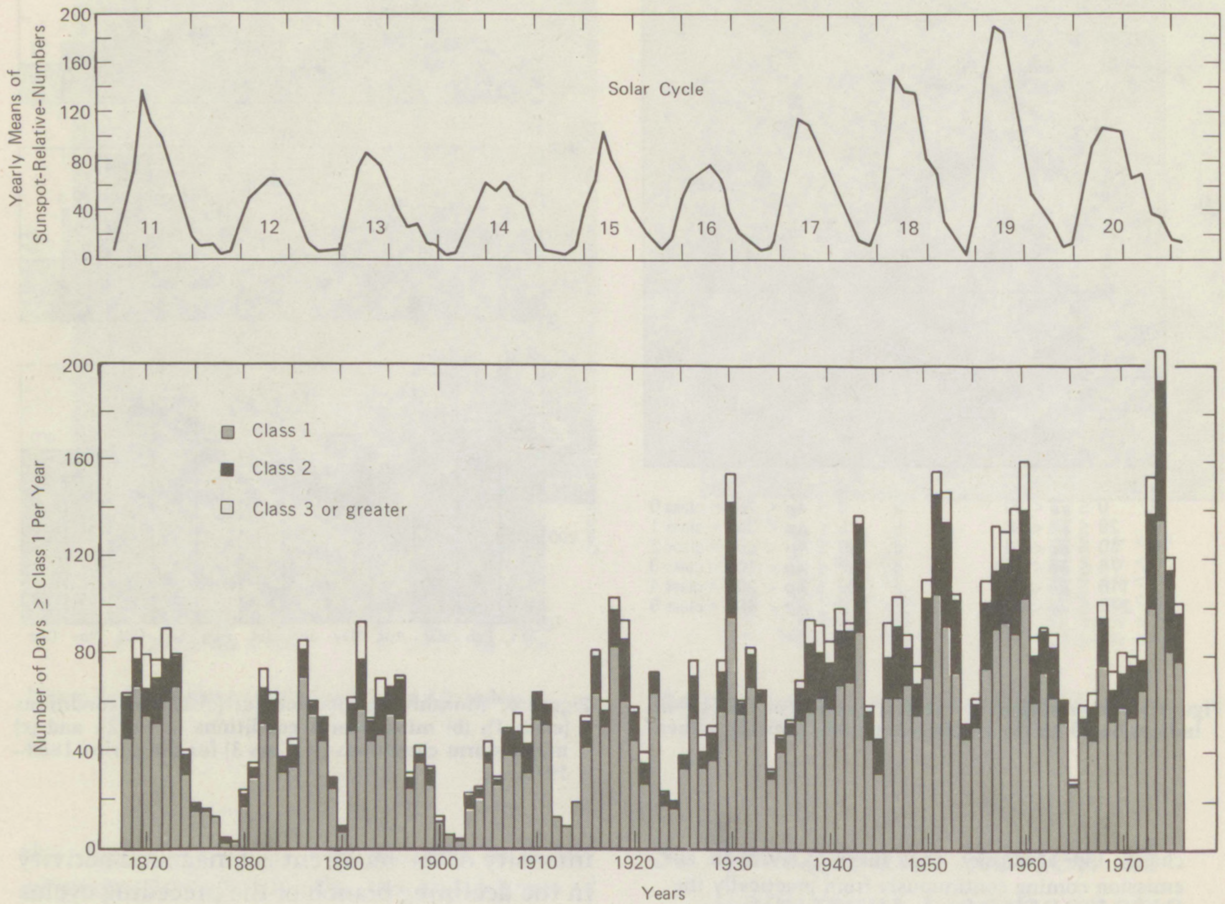

Figure 7. Annual distribution of geomagnetically disturbed days for the period 1868–1976: active (class 1), minor-storm (class 2), and major-storm (≥ class 3) conditions. Curve of yearly means of sunspot-relative-numbers is shown for comparison.

A graphical summary of the distribution of the class divisions of geomagnetic activity is presented as Figure 6, which shows the monthly totals for active, minor-storm, and major-storm conditions. Of interest is the persistency of the seasonal effect for all three levels of geomagnetic activity. This is evidence for the "semi-annual wave" phenomenon (see Section 2). However, analysis of the 109-year period shows this effect to be true for a long period, but it is not evident in each particular year.

Figure 7 shows the annual distribution for active, minor-storm, and major-storm conditions for the 1868–1976 period. The curve of the yearly means of sunspot-relative-numbers (Waldmeier, 1961) is added for comparison. Solar cycles 11, 13, 15, and 19 have a generally symmetrical pattern, whereas an asymmetrical pattern is exhibited by solar cycles 12, 14, 16, 17, 18, and 20. Except for cycle 18, these 10 solar cycles have exhibited alternating high-low relative sunspot maxima and, except for cycle 17, an alternating symmetrical-asymmetrical pattern in geomagnetic responses. The distribution depicted in Figure 7, however, does not describe the geomagnetic field response attributable to recurrent and nonrecurrent activity.

The interaction between the solar wind stream and Earth's geophysical environment is complex, and extensive research is currently in progress. If coronal holes are the main contributors to recurrent geomagnetic disturbances, then the classic M-regions provide a signature for the identification of the existence of past coronal holes. An analysis of the 109-year

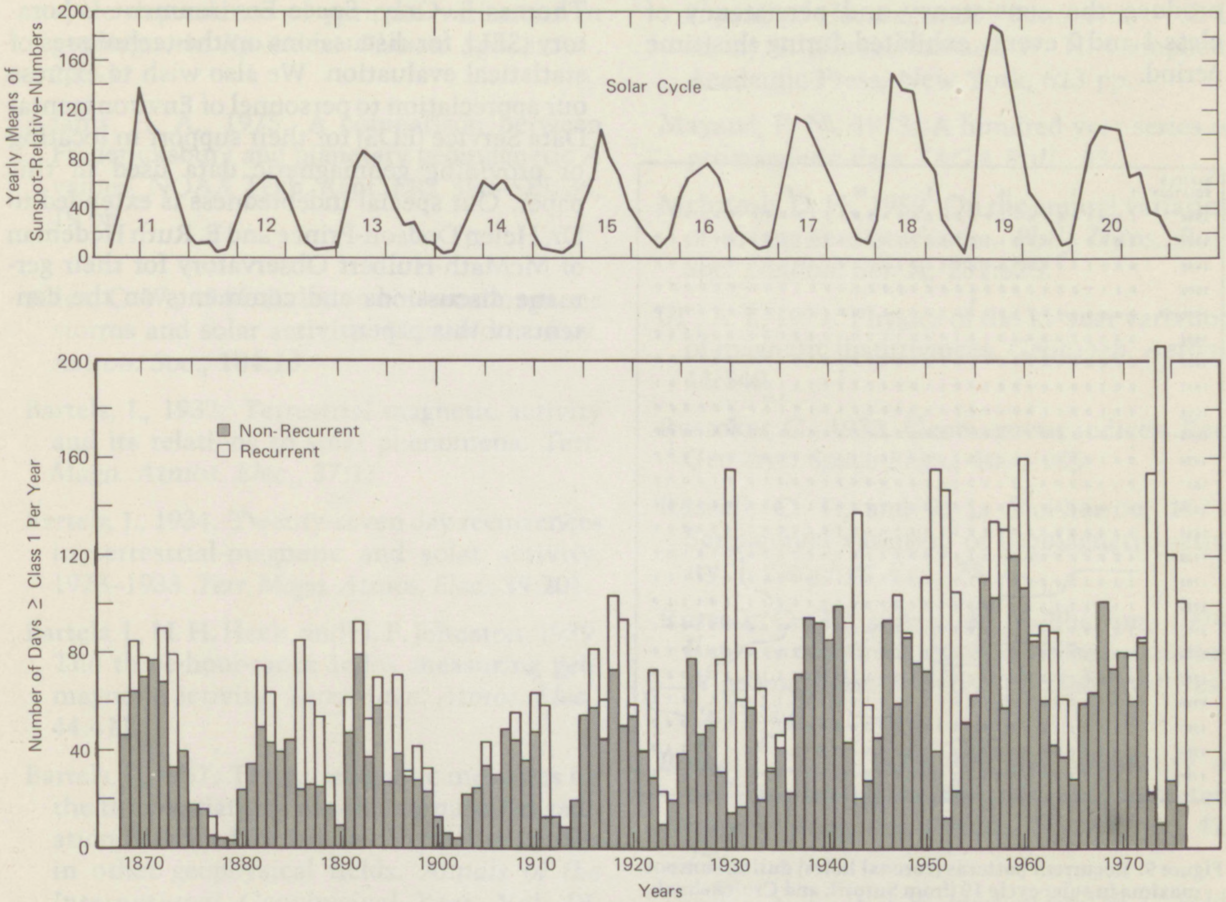

Figure 8. Annual distribution of geomagnetically disturbed days (≥ class 1) for the period 1868–1976: recurrent and nonrecurrent days. Curve of yearly means of sunspot-relative-numbers is shown for comparison.

period of class divisions for active- or storm-days (Sutorik and Cruickshank, 1977) identified 79 probable coronal holes. Three more were not included in the statistics because of doubtful signatures. Figure 8 shows the annual distribution of recurrent and nonrecurrent days based on these analyses. No attempt was made to remove obvious flare-related magnetically disturbed days from within an established recurrent pattern. For example, a class-5 event occurred on Bartels rotation 1705 in the midst of an assigned coronal hole structure. This depiction of the recurrent and nonrecurrent geomagnetic activity superbly illustrates the relationship discovered by Professor 01′. Even the consecutively increasing sunspot maxima for cycles 17, 18, and 19 obey the "01′ Law." Dodson et al. (1974) provide a detailed review of cycles 18, 19, and 20.

In an asymmetric cycle, coronal holes dominate the geomagnetic activity during the declining branch of a solar cycle. But this portion of a solar cycle is not the exclusive domain of coronal holes. Coronal holes have existed throughout each of the past 10 cycles. The longest-lived coronal hole shown by recurrent geomagnetic disturbances existed for 30 Bartels rotations (Nos. 1766–1796) occurring in 1962–1964. Very complex coronal hole structures would have existed during the following periods: 1929–1931 (Nos. 1320–1341), 1951–1952 (Nos. 1616–1634), and 1973–1974 (Nos. 1916–1942). Coronal holes were assigned to a geomagnetically disturbed period in 1957–1958

(Nos. 1701–1709) during the sunspot maxima of solar cycle 19 (Figure 9). It is difficult to accept the hypothesis that a flare-rich Sun could produce the consistency and persistency of class 1 and 2 events exhibited during this time period.

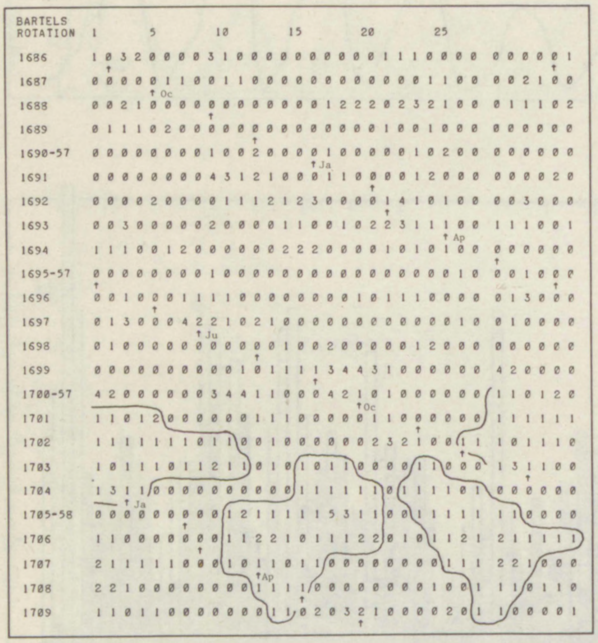

Figure 9. Recurrent patterns (coronal holes) during sunspot maxima in solar cycle 19 (from Sutorik and Cruickshank, 1977).

5. Conclusion

If the solar/geomagnetic characteristics exhibited through the last 10 solar cycles persist, the relationship shown by Professor 01′ implies there will be a marked increase in the annual mean relative sunspot number maximum for cycle 21. Also, if the alternating nature of the solar cycles continues, cycle 21 will be dominated by nonrecurrent geomagnetic disturbances with the frequency of occurrences following the rise and fall of the relative sunspot number. This dominance by nonrecurrent (flare-induced) disturbances as projected by this paper will make long-range forecasting of specific geomagnetically disturbed days or periods extremely difficult.

6. Acknowledgments

We wish to express our appreciation to Thomas B. Gray, Space Environment Laboratory (SEL), for discussions on the techniques of statistical evaluation. We also wish to express our appreciation to personnel of Environmental Data Service (EDS) for their support in locating or providing geomagnetic data used in this paper. Our special indebtedness is extended to Dr. Helen Dodson-Prince and E. Ruth Hedeman of McMath-Hulbert Observatory for their germane discussions and comments on the contents of this paper.

7. References

Abdel-Wahab, S. and A. Goned, 1974. Solar cycle dependence of periodic variations in geomagnetic *Kp*-index. *Planet. Space Sci.*, **22**:537.

Adams, H. A., 1975. A comparison between Fredericksburg and planetary geomagnetic *A* values. NOAA Tech. Rept. ERL 350–SEL 36, 19 pp.

Allen, C. W., 1944. Relation between magnetic storms and solar activity. *Mon. Notic. Roy. Astron. Soc.*, **104**:13.

Bartels, J., 1932. Terrestrial magnetic activity and its relations to solar phenomena. *Terr. Magn. Atmos. Elec.*, **37**:1.

Bartels, J., 1934. Twenty-seven day recurrences in terrestrial-magnetic and solar activity, 1923–1933. *Terr. Magn. Atmos. Elec.*, **39**:201.

Bartels, J., N. H. Heck, and H. F. Johnston, 1939. The three-hour-range index measuring geomagnetic activity. *Terr. Magn. Atmos. Elec.*, **44**:411.

Bartels, J., 1957. The geomagnetic measures for the time-variations of solar corpuscular radiation described for use in correlation studies in other geophysical fields. *Annals of the International Geophysical Year*, Vol. IV, Pergamon Press, London, 10 pp.

Bartels, J., 1963. Discussion of time-variations of geomagnetic activity indices *Kp* and *Ap*, 1932–1961. *Ann. Geophys.*, **19**:1.

Cage, A. L., and E. J. Zawalik, 1972. A discussion of the geomagnetic indices *Kp* and *Ap*, 1932 to 1971. AFCRL Environmental Research Papers, No. 423, 36 pp.

Chapman, S., and J. Bartels, 1940. *Geomagnetism*, Vol. I, Chap. 11, Oxford University Press, London, 542 pp.

Dodson, H. W., E. R. Hedeman, and D. C. Mohler, 1974. Comparison of activity in solar cycles 18, 19, and 20. *Rev. Geophys. Space Sci.*, **12**(3):329.

Kreiger, A. S., A. F. Timothy, and E. C. Roelof, 1973. A coronal hole and its identification as the source of a high velocity solar wind stream. *Solar Phys.*, **29**:505.

Lincoln, J. V., 1967. Geomagnetic indices. In: *Physics of Geomagnetic Phenomena*, Vol. I, ed. by S. Matsushita and W. H. Campbell, Academic Press, New York, 623 pp.

Mayaud, P. N., 1973. A hundred-year series of geomagnetic data. *IAGA Bull.*, **33**.

McIntosh, D. H., 1959. On the annual variation of magnetic disturbance. *Phil. Trans. Roy. Soc. London, Ser. A*, **251**:525.

01′, A. I., 1971. Physics of the 11-year variation of magnetic disturbances. *Geomagn. Aeron.*, **11**:549.

Rostoker, G., 1972. Geomagnetic indices. *Rev. Geophys. Space Phys.*, **10**(4):935.

Russell, C. T., and R. L. McPherron, 1973. Semiannual variation of geomagnetic activity. *J. Geophys. Res.*, **78**:92.

Russell, C. T., and R. L. McPherron, 1974. Reply to comment on "Semiannual variation of geomagnetic activity." *J. Geophys. Res.*, **79**:1132.

Russell, C. T., 1975. On the possibility of deducing interplanetary and solar parameters from geomagnetic records. *Solar Phys.*, **42**: 259.

Sheeley, N. R., Jr., J. W. Harvey, and W. C. Feldman, 1976. Coronal holes, solar wind streams, and recurrent geomagnetic disturbances: 1973–1976. *Solar Phys.*, **49**: 271.

Sutorik, J. A., and C. M. Cruickshank, 1977. Catalog of geomagnetic activity based on six class divisions, 1868–1976. NOAA Tech. Memo. ERL SEL–47.

Svalgaard, L., 1975. On the causes of geomagnetic activity. Stanford University, Institute for Plasma Research Report No. 646.

Waldmeier, M., 1961. The sunspot-activity in the years 1610–1960. Zurich Schulthess, Zurich, Switzerland, 171 pp.

Wilcox, J. M., 1968. The interplanetary magnetic field, solar origin and terrestrial effects. *Space Sci. Rev.*, **8**(2):258.

Appendix: Data Base and Data Sources

Data Base

Date	$\overline{aa}$	*Ap*	*Afr*	Date	$\overline{aa}$	*Ap*	*Afr*
21 Apr 37	21	12	15	23 Apr 39	93	92	65
22 Apr 37	8	4	4	24 Apr 39	96	79	89
23 Apr 37	12	6	6	25 Apr 39	80	61	52
24 Apr 37	52	45	47	12 Aug 39	88	88	82
25 Apr 37	69	72	47	13 Aug 39	43	34	26
26 Apr 37	90	67	61	14 Aug 39	20	9	9
27 Apr 37	55	61	53	15 Aug 39	9	5	4
28 Apr 37	135	130	106	16 Aug 39	73	62	36
29 Apr 37	32	19	11	17 Aug 39	27	20	16
30 Apr 37	29	21	13	21 Aug 39	15	9	8
01 Oct 37	40	29	23	22 Aug 39	103	135	74
02 Oct 37	9	7	7	23 Aug 39	86	89	55
03 Oct 37	33	25	20	24 Aug 39	27	13	18
04 Oct 37	61	71	69	23 Mar 40	49	51	33
05 Oct 37	16	8	5	24 Mar 40	223	190	138
06 Oct 37	17	10	11	25 Mar 40	242	185	179
07 Oct 37	34	23	19	26 Mar 40	44	53	37
08 Oct 37	47	38	42	27 Mar 40	38	30	26
09 Oct 37	54	42	32	28 Mar 40	29	21	23
10 Oct 37	61	38	28	29 Mar 40	102	100	76
11 Oct 37	55	46	45	30 Mar 40	180	190	189
12 Oct 37	43	30	23	31 Mar 40	134	130	102
13 Oct 37	21	14	10	01 Apr 40	67	66	53
14 Oct 37	18	13	12	02 Apr 40	35	34	19
15 Oct 37	36	20	12	03 Apr 40	89	98	81
12 Jan 38	30	15	12	04 Apr 40	23	15	15
13 Jan 38	40	29	30	01 Mar 41	250	205	219
14 Jan 38	14	9	6	02 Mar 41	55	35	25
15 Jan 38	22	9	11	03 Mar 41	36	26	21
16 Jan 38	58	34	30	04 Mar 41	55	40	31
17 Jan 38	139	120	109	05 Mar 41	48	37	28
18 Jan 38	46	34	31	28 Mar 41	77	59	39
19 Jan 38	36	24	18	29 Mar 41	53	42	30
20 Jan 38	40	25	21	30 Mar 41	94	85	57
21 Jan 38	63	38	35	31 Mar 41	86	76	48
22 Jan 38	240	130	131	04 Jul 41	35	26	24
23 Jan 38	25	16	14	05 Jul 41	303	220	236
24 Jan 38	37	16	11	06 Jul 41	60	42	30
25 Jan 38	189	105	154	07 Jul 41	59	54	41
26 Jan 38	82	62	52	08 Jul 41	26	14	15
27 Jan 38	23	12	11	13 Sep 41	32	24	17
01 Feb 38	27	13	7	14 Sep 41	39	24	24
02 Feb 38	21	13	11	15 Sep 41	40	26	22
03 Feb 38	33	16	14	16 Sep 41	28	20	22
04 Feb 38	28	13	10	17 Sep 41	19	10	9
05 Feb 38	17	9	9	18 Sep 41	350	230	238
06 Feb 38	67	51	32	19 Sep 41	199	175	188
07 Feb 38	41	24	20	20 Sep 41	42	36	26
08 Feb 38	56	36	27	21 Sep 41	44	30	30
09 Feb 38	54	32	29	22 Sep 41	7	4	6
10 Feb 38	43	31	20	23 Sep 41	25	14	11
11 Feb 38	37	27	26	24 Sep 41	35	27	25
12 Feb 38	19	10	8	25 Sep 41	30	22	18
13 Feb 38	25	16	13	01 Mar 42	147	110	90
14 Feb 38	54	39	26	02 Mar 42	46	45	32
11 May 38	120	105	99	03 Mar 42	49	42	26
12 May 38	81	76	80	04 Mar 42	26	17	13
13 May 38	14	17	22	05 Mar 42	58	52	33
14 May 38	55	40	32	06 Mar 42	28	24	24
15 May 38	35	24	20	07 Mar 42	39	19	19
14 Sep 38	59	49	29	08 Mar 42	51	39	28
15 Sep 38	117	100	65	09 Mar 42	52	41	30
26 Sep 38	58	38	26	10 Mar 42	28	15	12
27 Sep 38	40	30	18	11 Oct 42	21	10	11
28 Sep 38	62	56	33	12 Oct 42	50	36	30
29 Sep 38	28	16	16	13 Oct 42	44	32	27
30 Sep 38	47	32	18	14 Oct 42	43	34	30
17 Apr 39	147	135	124	15 Oct 42	43	26	25
18 Apr 39	48	42	28	16 Oct 42	37	22	20
19 Apr 39	65	45	28	17 Oct 42	21	14	16
20 Apr 39	34	27	24	18 Oct 42	30	19	15

Data Sources

1. **Solar-Geophysical Data series (NOAA/EDS) and its predecessors, 1956–1975.**
2. **International Association for Geomagnetism and Aeronomy (IAGA) Bulletin series.**
3. **Terrestrial Magnetism and Atmospheric Electricity, Vols. 44, 45, 46.**

Date	$\overline{aa}$	*Ap*	*Afr*
19 Oct 42	43	33	30
20 Oct 42	27	19	12
28 Oct 42	59	56	25
29 Oct 42	85	80	76
30 Oct 42	48	39	32
31 Oct 42	45	30	32
07 Feb 46	184	125	137
08 Feb 46	134	120	82
24 Mar 46	100	115	89
25 Mar 46	195	195	118
26 Mar 46	52	51	35
27 Mar 46	36	30	23
28 Mar 46	322	215	244
29 Mar 46	42	35	28
26 Jul 46	95	79	58
27 Jul 46	131	150	145
16 Sep 46	40	34	17
17 Sep 46	38	29	28
18 Sep 46	117	135	95
19 Sep 46	54	58	32
20 Sep 46	16	14	10
21 Sep 46	31	22	17
22 Sep 46	272	200	204
23 Sep 46	141	145	97
24 Sep 46	29	21	17
25 Sep 46	7	5	4
26 Sep 46	10	7	7
27 Sep 46	57	38	22
28 Sep 46	95	91	49
29 Sep 46	43	36	21
30 Sep 46	38	35	28
26 Apr 56	54	40	35
27 Apr 56	159	172	192
28 Apr 56	50	64	48
29 Apr 56	57	58	37
30 Apr 56	57	51	32
12 May 56	55	38	38
13 May 56	54	34	27
14 May 56	24	16	13
15 May 56	49	42	27
16 May 56	129	156	115
17 May 56	54	52	35
18 May 56	13	9	11
19 May 56	13	9	8
20 May 56	42	39	32
21 May 56	21	16	20
22 May 56	29	18	16
23 May 56	35	28	18
24 May 56	92	95	72
25 May 56	58	69	50
10 Nov 56	72	62	40
11 Nov 56	70	72	51
12 Nov 56	68	48	27
13 Nov 56	21	16	10
14 Nov 56	57	59	34
15 Nov 56	99	86	45
21 Jan 57	130	82	73
22 Jan 57	95	70	37
02 Mar 57	154	132	105
29 Mar 57	109	77	44
02 Sep 57	96	102	63
03 Sep 57	159	135	94
04 Sep 57	160	145	117
05 Sep 57	101	112	109
13 Sep 57	163	160	143
21 Sep 57	78	74	41
22 Sep 57	118	104	63
23 Sep 57	184	164	109
24 Sep 57	41	33	23
29 Sep 57	131	139	74
30 Sep 57	66	56	28
11 Feb 58	298	199	204
12 Feb 58	97	59	44
08 Jul 58	305	200	178
09 Jul 58	66	75	41
04 Sep 58	162	131	86
05 Sep 58	70	71	52
26 Mar 59	85	81	52
27 Mar 59	166	178	123
15 Jul 59	347	236	225
16 Jul 59	47	47	32
17 Jul 59	135	110	101
18 Jul 59	96	119	80
16 Aug 59	138	130	69
17 Aug 59	96	114	76
21 Sep 59	100	86	44
28 Nov 59	100	82	58
05 Dec 59	92	68	33
31 Mar 60	144	129	96
01 Apr 60	299	241	182
30 Apr 60	202	174	160
08 May 60	114	128	77
04 Sep 60	94	95	59
05 Sep 60	114	118	89
06 Oct 60	219	203	115
07 Oct 60	164	186	119
08 Oct 60	47	33	20
25 Oct 60	94	76	34
26 Oct 60	73	63	37
27 Oct 60	52	38	33
11 Nov 60	36	18	14
12 Nov 60	106	67	46
13 Nov 60	352	280	264
14 Nov 60	60	49	35
15 Nov 60	86	69	48
16 Nov 60	127	94	47
17 Nov 60	27	18	18
11 Sep 63	38	20	16
12 Sep 63	25	13	15
13 Sep 63	15	8	7
14 Sep 63	95	82	42
15 Sep 63	59	38	27
16 Sep 63	54	33	26
17 Sep 63	58	43	28
18 Sep 63	28	15	10
19 Sep 63	49	26	19
20 Sep 63	20	13	10
21 Sep 63	50	44	25
22 Sep 63	134	126	74
23 Sep 63	100	78	80
24 Sep 63	31	18	11
25 Sep 63	81	60	29
26 Sep 63	39	27	17
27 Sep 63	50	34	22
28 Sep 63	60	48	30
29 Sep 63	34	19	16
30 Aug 66	91	82	42
31 Aug 66	34	23	16
01 Sep 66	36	22	15
02 Sep 66	29	15	13
03 Sep 66	86	92	45
04 Sep 66	80	112	79
05 Sep 66	24	13	12
24 May 67	21	11	11
25 May 67	148	130	112
26 May 67	168	146	156
27 May 67	36	20	16
28 May 67	63	55	35
29 May 67	53	45	35
30 May 67	57	42	37
31 May 67	46	43	34

Environmental Research LABORATORIES

The mission of the Environmental Research Laboratories (ERL) is to conduct an integrated program of fundamental research, related technology development, and services to improve understanding and prediction of the geophysical environment comprising the oceans and inland waters, the lower and upper atmosphere, the space environment, and the Earth. The following participate in the ERL missions:

MESA *Marine EcoSystems Analysis Program.* Plans, directs, and coordinates the regional projects of NOAA and other federal agencies to assess the effect of ocean dumping, municipal and industrial waste discharge, deep ocean mining, and similar activities on marine ecosystems.

OCSEA *Outer Continental Shelf Environmental Assessment Program Office.* Plans and directs research studies supporting the assessment of the primary environmental impact of energy development along the outer continental shelf of Alaska; coordinates related research activities of federal, state, and private institutions.

WM *Weather Modification Program Office.* Plans, directs, and coordinates research within ERL relating to precipitation enhancement and mitigation of severe storms. Its National Hurricane and Experimental Meteorology Laboratory (NHEML) studies hurricane and tropical cumulus systems to experiment with methods for their beneficial modification and to develop techniques for better forecasting of tropical weather. The Research Facilities Center (RFC) maintains and operates aircraft and aircraft instrumentation for research programs of ERL and other government agencies.

AOML *Atlantic Oceanographic and Meteorological Laboratories.* Studies the physical, chemical, and geological characteristics and processes of the ocean waters, the sea floor, and the atmosphere above the ocean.

PMEL *Pacific Marine Environmental Laboratory.* Monitors and predicts the physical and biological effects of man's activities on Pacific Coast estuarine, coastal, deep-ocean, and near-shore marine environments.

GLERL *Great Lakes Environmental Research Laboratory.* Studies hydrology, waves, currents, lake levels, biological and chemical processes, and lake-air interaction in the Great Lakes and their watersheds; forecasts lake ice conditions.

GFDL *Geophysical Fluid Dynamics Laboratory.* Studies the dynamics of geophysical fluid systems (the atmosphere, the hydrosphere, and the cryosphere) through theoretical analysis and numerical simulation using powerful, high-speed digital computers.

APCL *Atmospheric Physics and Chemistry Laboratory.* Studies cloud and precipitation physics, chemical and particulate composition of the atmosphere, atmospheric electricity, and atmospheric heat transfer, with focus on developing methods of beneficial weather modification.

NSSL *National Severe Storms Laboratory.* Studies severe-storm circulation and dynamics, and develops techniques to detect and predict tornadoes, thunderstorms, and squall lines.

WPL *Wave Propagation Laboratory.* Studies the propagation of sound waves and electromagnetic waves at millimeter, infrared, and optical frequencies to develop new methods for remote measuring of the geophysical environment.

ARL *Air Resources Laboratories.* Studies the diffusion, transport, and dissipation of atmospheric pollutants; develops methods of predicting and controlling atmospheric pollution; monitors the global physical environment to detect climatic change.

AL *Aeronomy Laboratory.* Studies the physical and chemical processes of the stratosphere, ionosphere, and exosphere of the Earth and other planets, and their effect on high-altitude meteorological phenomena.

SEL *Space Environment Laboratory.* Studies solar-terrestrial physics (interplanetary, magnetospheric, and ionospheric); develops techniques for forecasting solar disturbances; provides real-time monitoring and forecasting of the space environment.

U.S. DEPARTMENT OF COMMERCE
National Oceanic and Atmospheric Administration
BOULDER, COLORADO 80302